Journal of Power Sources 203 (2012) 103–108

Contents lists available at SciVerse ScienceDirect

Journal of Power Sources

journal homepage: www.elsevier.com/locate/jpowsour

Mechanism on exothermic heat of FeF_3 cathode in Li-ion batteries

Mingjiong Zhou [a,*], Liwei Zhao [b], Ayuko Kitajou [b], Shigeto Okada [b], Jun-ichi Yamaki [b]

[a] Interdisciplinary Graduate School of Engineering Sciences, Kyushu University, 6-1 Kasaga-koen, Kasuga 816-8580, Japan
[b] Institute for Materials Chemistry and Engineering, Kyushu University, 6-1 Kasaga-koen, Kasuga 816-8580, Japan

ARTICLE INFO

Article history:
Received 29 October 2011
Received in revised form 7 December 2011
Accepted 8 December 2011
Available online 17 December 2011

Keywords:
FeF_3
Cathode
Exothermic heat
Mechanism
Lithium-ion battery

ABSTRACT

To identify the mechanism of exothermic reactions of cycled FeF_3 electrodes in an electrolyte with temperature ramp-up, the structure and thermal behavior of cycled FeF_3 electrodes were investigated using a combination of XRD and DSC. The combination of XRD and DSC revealed that FeF_3 can be restored and the electrochemical was reversible even after the conversion reaction. In the discharged electrodes, a structural transformation to $LiFeF_3$ was observed after 1Li insertion, and two compounds (LiF and Fe metal) were formed during the conversion reaction. Accordingly, the differences of thermal behavior in the electrolyte were presented in the DSC curves. It was clear that no reaction occurred between LiF and the electrolyte at elevated temperatures. In contrast, Fe powder was found to react with the electrolyte at around 300 °C, indicating that Fe metal generated in the electrode had a direct effect on the thermal behavior of the discharged FeF_3 electrode. Moreover, Fe powder was found to react with PF_5 produced by $LiPF_6$ decomposition. The mixture of discharged FeF_3 electrode and electrolyte showed less heat generation than the electrolyte alone because some PF_5 was consumed by the generated Fe metal in the electrode.

1. Introduction

Rechargeable lithium-ion batteries with high energy density and potential have been used in a wide variety of portable electronic devices. They are now being investigated as possible power sources for hybrid electric vehicles and electric vehicles [1–6]. However, the use of Li-ion batteries in this application has been limited due to safety concerns associated with the thermal stability of their constituent materials [2–9]. Exothermic reactions such as the reaction between electrode and electrolyte and the decomposition of electrolyte in the battery can cause thermal runaway if the heat output exceeds the thermal diffusion [9,10]. A number of researchers have performed experiments on individual electrodes in electrolyte to propose possible mechanism of the exothermic reactions at elevated temperatures by using differential scanning calorimetry (DSC) [1–6] and accelerated rate calorimetry (ARC) [11–15].

The 3d-transition-metal binary compounds M_xX_y (M = Co, Cu, Fe, etc.; X = F, O, S, etc.) have been extensively studied as electrode materials for Li-ion batteries. Tarascon's group first revealed that these materials attained the highest specific capacities by utilizing all the possible oxidation states of compound during the redox cycle [16]. This can be done by way of a reversible conversion reaction of the form

$$M_xX_y + nyLi \rightleftarrows yLi_nX + xM \quad (1)$$

Among these M_xX_y materials, metal fluorides can be used as alternative cathode materials for Li-ion batteries because of the high voltages due to their highly ionic character [17–25]. Metal fluorides enable the highest specific capacity via the reversible conversion process through the following reaction scheme [17,18]:

$$xLi^+ + xe^- + MeF_x \rightleftarrows xLiF + Me \quad (2)$$

However, metal fluorides have poor electronic conductivity due to their wide energy gap. To overcome this problem, highly conductive carbon such as acetylene black was mixed with the metal fluorides by ball-milling to enhance the electrochemical activity and achieve satisfied reversibility during cycling. In the case of FeF_3, the discharged capacity of 80 mAh g^{-1} between 2.0 and 4.5 V involved in the Fe^{3+}/Fe^{2+} redox reaction was first reported by Arai et al. [19]. By using highly conductive carbon, the electrochemical activity was improved, and about 99% of the FeF_3 theoretical capacity (235 vs. 237 mAh g^{-1}) in the 2.0–4.5 region was achieved [5,20–24]. Amatucci's group subsequently demonstrated a reversible conversion of FeF_3 electrodes with appreciable energy capacity [17,18,22]. They have proposed the following reaction schemes:

$$FeF_3 + Li \rightarrow LiFeF_3 \quad (4.5\text{–}2.5\,V) \quad (3)$$

* Corresponding author. Tel.: +81 92 583 7791; fax: +81 92 583 7791.
E-mail address: m-zhou@cm.kyushu-u.ac.jp (M. Zhou).

0378-7753/$ – see front matter © 2011 Elsevier B.V. All rights reserved.
doi:10.1016/j.jpowsour.2011.12.016

$$LiFeF_3 + 2Li \rightarrow 3LiF + Fe \quad (2.5\text{–}1.5\,V) \tag{4}$$

In the region of 4.5–2.5 V (Eq. (3)), Li-ions are inserted into the FeF_3 framework to form a $LiFeF_3$ phase. This process appears to be fully reversible, because FeF_3 adopts a perovskite structure, which contains vacant sites available for Li-ion insertion. In the subsequent step (Eq. (4)), $LiFeF_3$ decomposes to form LiF and Fe metal, which are on the scale of 2–5 nm [18]. This enables high specific capacities of FeF_3 approaching 700 mAh g^{-1} at energy densities exceeding 1200 Wh kg^{-1}, which provides an avenue to a high-specific-capacity cathode in applications for Li-ion batteries. However, this outstanding specific capacity of a FeF_3 mixed with highly conductive carbon was only attainable at mild operating conditions of low current density and elevated temperature. To improve the electrochemical activity of the FeF_3 cathode for further practical applications, a new hierarchical nanostructure composed of FeF_3 nanoparticles and carbon nanotubes (CNTs) was fabricated by Kim et al. [25], and this CNT–FeF_3 composite showed superior electrochemical performance at a high current rate. Due to the outstanding improvement of the electrochemical performance, FeF_3 becomes an attractive cathode material for vehicle power supply.

From the point of practical application, the thermal stability of the FeF_3 cathode must be investigated because it is crucial for the safety of Li-ion batteries. We previously studied the thermal stability of FeF_3 electrodes via the insertion or conversion reaction using differential scanning calorimetry (DSC) [5,6]. For the cycled FeF_3 electrodes via the insertion or conversion reaction, both charged and discharged electrodes decomposed at high temperatures above 300 °C, indicating that the FeF_3 electrode had great thermal stability at elevated temperatures. In addition, the thermal stability of FeF_3 electrodes in a 1 M $LiPF_6$/EC + DMC electrolyte was studied by changing the ratio of cycled electrode to electrolyte. As a result, differences of the thermal behavior in the electrolyte between charged and discharged FeF_3 electrodes were observed. The charged electrodes via the insertion or conversion reaction gave similar thermal behavior in the electrolyte at elevated temperatures. For the discharged FeF_3 electrodes, the thermal stability of discharged FeF_3 electrodes in the electrolyte increased after the conversion reaction. This different thermal behavior for the electrode would normally be attributed to the variation of the electrode composition, but the heat generation of the mixtures of the cycled FeF_3 electrodes and electrolyte was smaller than the electrolyte alone. Furthermore, it was found that the FeF_3 electrode showed better thermal stability than the $LiFePO_4$ electrode in the electrolyte.

To study the mechanism of exothermic reactions of cycled FeF_3 electrodes in the electrolyte, in combination with the previous research, the cycled FeF_3 electrodes were characterized using X-ray diffraction (XRD), and relative reference DSC measurements were carried out in this study.

2. Experimental

Commercially available FeF_3 ($d_{50\%}$ = 12 μm, Soekawa Chemical Co.) was used. The cathode was prepared by using the FeF_3, acetylene black and PTFE-binder (70:25:5 wt%). The fabrication method of pellets and FeF_3–cell construction were the same as described in the experimental sections of Refs. [5,6]. For 1Li insertion, the assembled cell was cycled at a constant current density of 0.2 mA cm^{-2} (ca. 7.5 mA g^{-1}) with an ending capacity of 237 mAh g^{-1} (theoretical capacity of FeF_3). For the 2Li or 3Li conversion, the charge–discharge measurements were the same as in the previous report [6]. After charge and discharge, the cells were disembled in an Ar-filled glove box. The cathodes were washed and dried following previously described methods [5,6]. The obtained electrodes were used for DSC and XRD measurements.

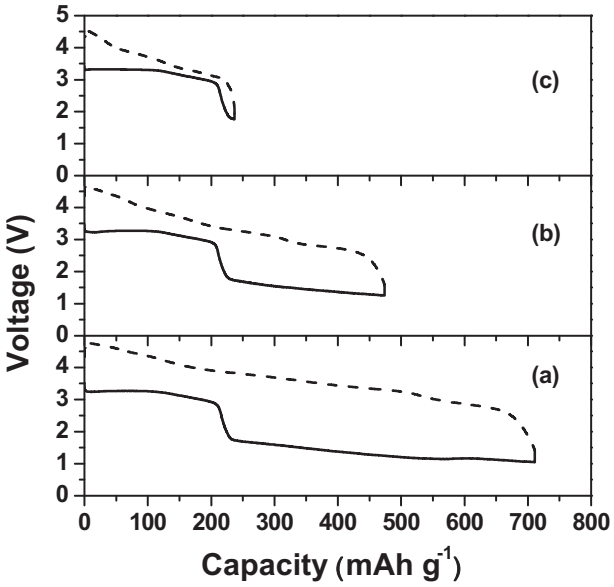

Fig. 1. Charge and discharge curves of a FeF_3 electrode in 1 M $LiPF_6$/EC + DMC electrolyte: (a) 3Li cycling; (b) 2Li cycling; (c) 1Li cycling.

Similar to the test electrodes, thermal analysis of commercially available Fe powder (100 nm dia., Japan Ion Co.) and LiF powder (Wako Pure Chemical Industries, Ltd.) were carried out by DSC. All the samples for DSC measurements were prepared in an Ar-filled glove box. The powder together with the electrolyte was packed in a crimp-sealed stainless pan, and then heated from room temperature to 500 °C at a heating rate of 5 °C min^{-1}. The TG signal was monitored simultaneously during data collection to confirm that the pan was hermetic.

To analyze the structure changes during cycling, the cycled electrodes were characterized by XRD (Rigaku RA-HF/18TTR3) utilizing Cu Kα radiation. A range of 2θ values from 10 to 80° with a scanning rate of 0.06° min^{-1} and a step size of 0.02° was applied. For comparison, a fresh electrode (tested before making a coin cell) was also probed using the same method. All the samples were under Ar atmosphere during the transfer and XRD measurements.

3. Results and discussion

The electrochemical performance of the FeF_3 electrodes was carried out using the coulostatic method, and the charge–discharge profiles are shown in Fig. 1. The cutoff capacities were set as 237, 474 and 711 mAh g^{-1}, respectively, corresponding to stoichiometrical 1Li, 2Li and 3Li insertion into the FeF_3 electrodes. For 1Li insertion, a flat plateau at 3.3 V was observed followed by a voltage drop to 1.8 V started at the capacity of 200 mAh g^{-1}, involving the Fe^{3+}/Fe^{2+} reduction reaction in this range (Eq. (3)). After that, the voltage mildly decreased to 1.1 V along with the capacity of 711 mAh g^{-1}, which was involved in the reduction of Fe^{2+} to Fe^0 (Eq. (4)). No voltage drop was visible in this range, indicating that the transfer process from Fe^{2+} to Fe^0 proceeded in a straightforward two-phase conversion reaction. The electrochemical behavior of the FeF_3 electrode was quite similar to the behavior found by Yamakawa as well that in our previous report [5,24], although a different cycling method was used in these studies. However, compared with Yamakawa's result, the first plateau at 3.3 V in the discharge curve was much flatter in our studies, presumably due to the different processes used to prepare the carbon–FeF_3 composites, such as the FeF_3/carbon ratio and ball-milling conditions. Additionally, the operating voltage was found to be close in both of these two studies, but was lower than that reported by Badway

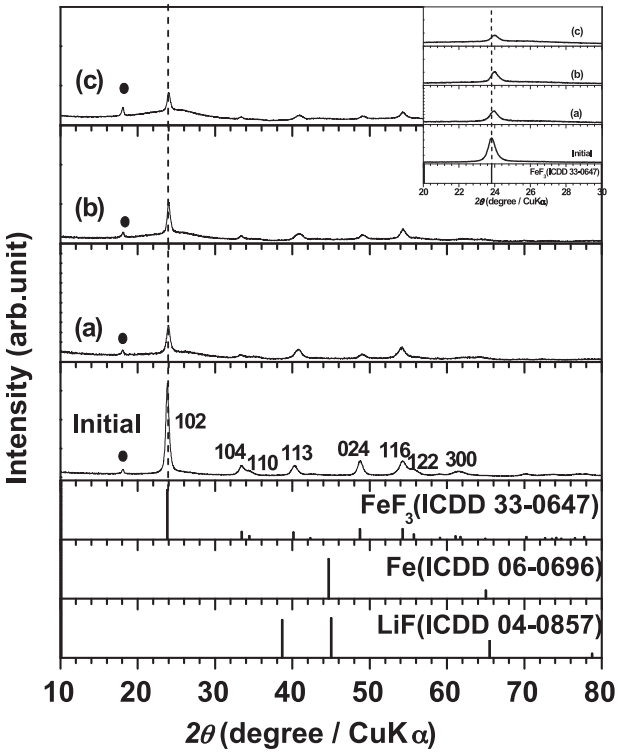

Fig. 2. XRD patterns of charged FeF_3 electrodes at various cycling depths: (a) after 1Li cycling; (b) after 2Li cycling; and (c) after 3Li cycling. The XRD reflection of the PTFE peak is marked by solid circle points.

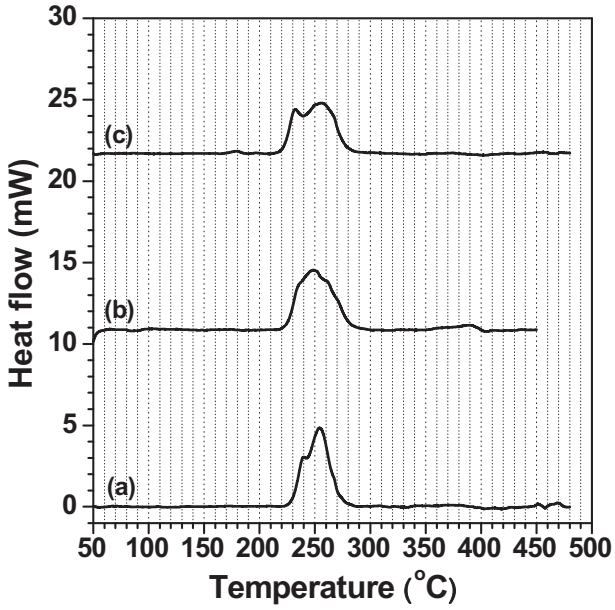

Fig. 3. DSC curves of mixtures of 4 μl electrolyte and charged FeF_3 electrodes. The electrodes were carried out at various cycling depths: (a) after 1Li cycling; (b) after 2Li cycling; and (c) after 3Li cycling.

et al. [21,22]. This phenomenon was probably due to the different temperature used in the studies, as suggested by Yamakawa et al. [24]. For the charge process, no noticeable plateau was observed, and the voltage profile was different from the discharge curve.

From the point of application, FeF_3 used as the active material of the cathode in rechargeable Li-ion battery should be reversible after the charge process. Therefore, the structure of charged electrodes at different depths was examined by XRD. Fig. 2 shows the XRD patterns of charged FeF_3 electrodes after various cycling depths, with the XRD pattern of a fresh electrode used as a reference. The XRD patterns of the charged electrodes were similar to that of the fresh sample. This observation indicated that the inserted Li-ions were almost fully extracted from the electrodes, and FeF_3 could be restored at the end of charging, which was consistent with the suggestion by Doe et al. [26]. This result combined with capacity data proved that the electrochemical reaction of the FeF_3 electrodes was reversible. Upon closer comparison, the XRD patterns of the charged electrodes exhibited some minor changes from the fresh one. All of the reflections for the charged samples became broader and weaker, indicating that the crystalline phase tended to deteriorate, perhaps due to formation of small particles during cycling. Additionally, the most intense reflection at $2\theta = 24^\circ$, corresponding to the (1 0 2) peak of the FeF_3 phase, slightly shifted to a higher angle and decreased in intensity with the increase of the cycling depth. The peak shift was probably caused by the structural shrinkage of the FeF_3 framework or formation of a defect trirutile structure instead of the rhombohedral structure as Doe supposed [26]. In summary, it was clear that FeF_3 can be restored after the charge process, but structural changes presumably occur. Similar results could be obtained from the data of DSC analysis. Fig. 3 shows the DSC curves of mixtures of 1 mg charged electrodes at various depths and 4 μl electrolyte (the data of the electrode in conversion states has been published previously [6]). The exothermic peak was observed in the range of 210–300 °C due to the reaction of the electrode with electrolyte and the electrolyte decomposition [5,6]. However, we found that the exothermic peak became much milder and the temperature range of the exothermic reaction tended to be wider with the increase of the cycling depth. As expected, this was probably because the structure of charged electrodes changed with the increase of the cycling depth.

In layered compounds (such as $LiCoO_2$), lithium is stored between the layers and lithium intercalation and deintercalation occur during the charge–discharge cycles without significant structural change [27]. However, 3d-transition-metal binary compounds (such as FeF_3) have a perovskite structure, which is easily changed after lithium insertion, particularly during the conversion reaction. To trace the structural evolution during the discharge process, the discharged FeF_3 electrodes were investigated by XRD.

Fig. 4 shows the XRD patterns of the discharged FeF_3 electrodes at various discharge depths, together with the XRD pattern of a fresh electrode as a reference. After discharged to 1Li, the reflections of (0 2 4), (1 0 4) and especially (1 0 2) dramatically decreased in intensity, and shifted to a lower angle. At the same time, two obvious peaks at $2\theta = 40$ and 53° were observed in the XRD pattern, as shown in Fig. 4a. Upon closer comparison, the peak at $2\theta = 40^\circ$ was found to be almost in the same position as the (1 1 3) peak at $2\theta = 40.5^\circ$, but was much more distinct in intensity. Regarding the peak at $2\theta = 53^\circ$, there was no peak in the XRD pattern of the fresh sample directly corresponding to it, except for the near peak of (1 1 6) at $2\theta = 54.5^\circ$. Yamakawa et al. [24] reported that the reflections of (1 1 3) and (1 1 6) gradually shifted to similar positions as those we found during Li insertion to Li = 1.0. Therefore, the peaks at $2\theta = 40$ and 53° in the present study should come from the reflections of (1 1 3) and (1 1 6), respectively. Additionally, the peak shift of (1 1 6) was larger than that of (1 1 3), suggesting an anisotropical crystal lattice in the perovskite structure of FeF_3. All of the observed changes can be attributed to Li insertion accompanied by formation of $LiFeF_3$. When the discharge depth increased to 2Li and 3Li, the reflections at $2\theta = 40$ and 53° gradually decreased, but remained till Li = 3.0, indicating that there was still a small amount of the $LiFeF_3$ phase left even after 3Li conversion. Simultaneously, two new reflections, which were identified as LiF and Fe metal, became visible in the XRD patterns as expected. With the increase of the

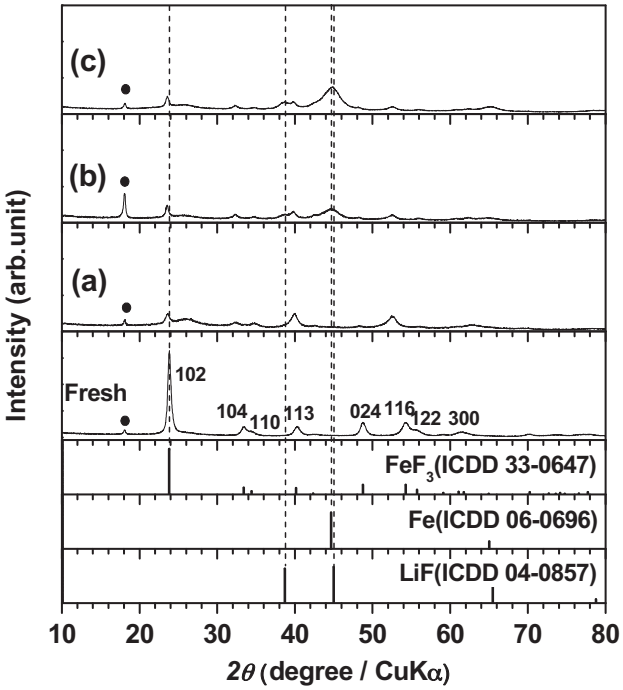

Fig. 4. XRD patterns of discharged FeF_3 electrodes at various discharge depths: (a) after 1Li insertion; (b) after 2Li conversion; and (c) after 3Li conversion. The XRD reflection of the PTFE peak is marked by solid circle points.

discharge depth, the reflections of LiF and Fe metal were found to significantly grow in intensity. This observation was consistent with the electrochemical reaction involved in reduction from Fe^{2+} to Fe^0. It should be pointed out that the sharp peak at $2\theta = 18^\circ$ in the XRD pattern for Li = 2.0 was caused by the concentration of PTFE.

The variation of the composition of discharged FeF_3 electrodes was also reflected from the thermal behavior of the discharged electrodes in the electrolyte. Fig. 5 compares the DSC curves of the discharged FeF_3 electrodes at various depths (1 mg) in the electrolyte (4 μl), while the data of the electrode in conversion states

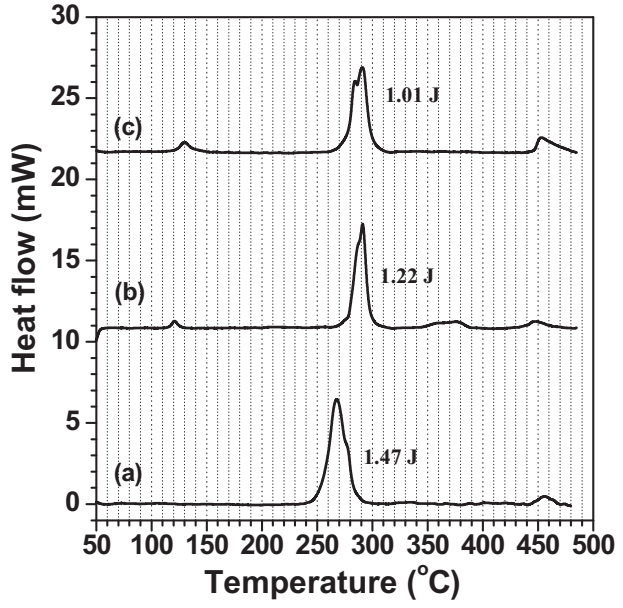

Fig. 5. DSC curves of mixtures of 4 μl electrolyte and discharged FeF_3 electrodes. The electrodes were carried out at various discharge depths: (a) after 1Li insertion; (b) after 2Li conversion; and (c) after 3Li conversion.

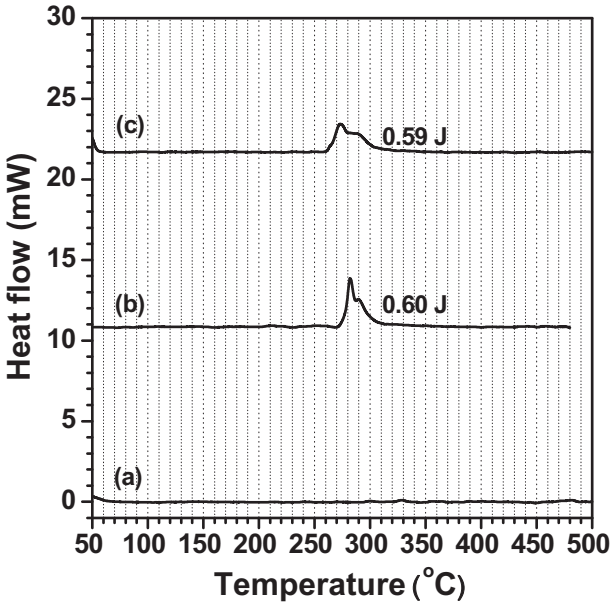

Fig. 6. DSC curves of (a) 1 mg LiF, (b) 1 μl of 1 M $LiPF_6$/EC + DMC electrolyte and (c) mixture of 1 mg LiF and 1 μl of 1 M $LiPF_6$/EC + DMC.

has been reported previously [6]. Obviously, the differences of thermal behavior were distinct for the discharged electrodes between the insertion and conversion states. A dominant exothermic peak was found to shift from 270 to 290 °C, although all of the peaks were due to the reaction of the electrode with electrolyte and the electrolyte decomposition [5,6]. Moreover, the dominant exothermic peak decreased with the increase of the discharge depth. The observed differences were likely related to the variation in the composition of electrode during the discharge process, because the composition of electrode transformed from $LiFeF_3$ to Fe metal and LiF, as detected by XRD. This assumption is examined by a detailed analysis on the thermal behavior of LiF and Fe metal below.

To identify the effect of the composition of discharged FeF_3 electrodes on their thermal stability, the thermal behavior of LiF and Fe powder in 1 M $LiPF_6$/EC + DMC electrolyte was investigated in detail by DSC with the same method as the FeF_3 electrodes. Fig. 6 shows the DSC curves of LiF powder, the electrolyte and mixture of LiF powder and the electrolyte. No noticeable peak was observed for LiF powder up to 500 °C, indicating that the LiF powder had a great thermal stability at elevated temperatures. When 1 mg LiF powder mixed with 1 μl of electrolyte was sealed in a pan, an exothermic peak at around 272 °C was observed, and the heat value was evaluated as 0.59 J by integrating the DSC curve. The thermal behavior of the mixture was quite similar to that of the 1 μl electrolyte, including the peak shape and peak position, and even the heat value was almost the same. Therefore, the exothermic peak at around 272 °C was caused by the electrolyte decomposition, rather than the reaction of LiF with electrolyte, suggesting that no reaction occurred between LiF and the electrolyte even at elevated temperatures.

Our group reported the thermal characteristics of FeF_3 electrodes in conversion states with the electrolyte at elevated temperatures [6]. The amount of Fe metal in the electrode was estimated to be ca. 0.3 mg based on 1 mg of discharged FeF_3 electrode in the conversion state. Moreover, the Fe metal generated in the discharged electrode after the conversion reaction has a rather small particle size. Therefore, 0.3 mg of nano-sized Fe powder was used for the reference analysis. Fig. 7 shows the DSC curves of mixtures of 0.3 mg Fe powder and given amounts of electrolyte (ranging from 0.5 to 5 μl). The DSC curve of 0.3 mg Fe powder is also presented in Fig. 7. When the amount of coexisting electrolyte was

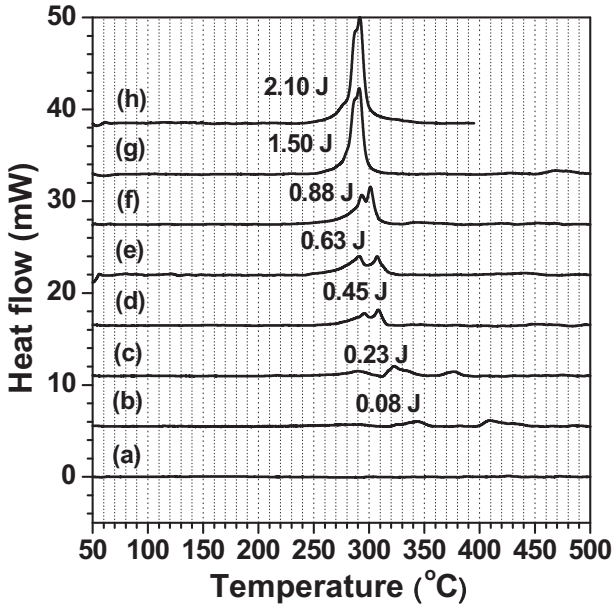

Fig. 7. DSC curves of (a) 0.3 mg of Fe powder and of mixtures of 0.3 mg Fe powder and (b) 0.5 μl, (c) 1 μl, (d) 2 μl, (e) 2.5 μl, (f) 3 μl, (g) 4 μl and (h) 5 μl of 1 M $LiPF_6$/EC + DMC electrolyte.

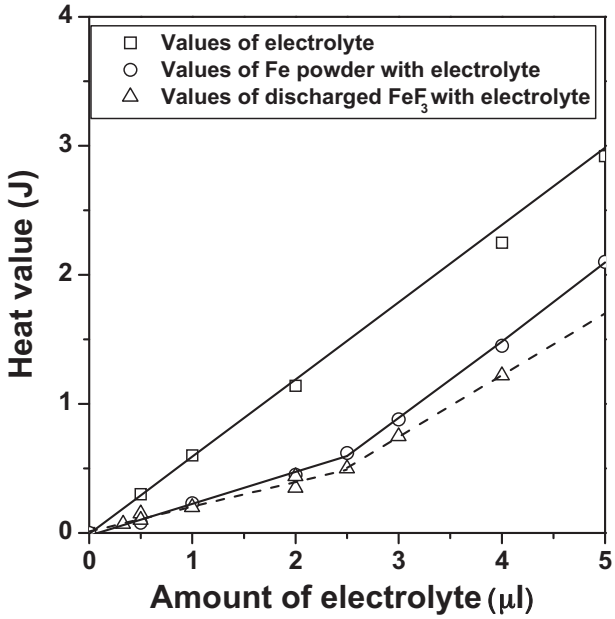

Fig. 8. Correlation between the heat values obtained for the mixtures and the amount of electrolyte sealed in a pan. The heat values were evaluated by integrating DSC curves at temperatures ranging from 250 to 360 °C. The dashed lines represent the tendency of heat generation from the mixtures of 1 mg discharged FeF_3 electrode in the conversion state and electrolyte.

0.5 and 1 μl, no obvious exothermic heat was observed from the DSC curves, even up to 500 °C. Only some small thermal fluctuations were detected at around 300 °C, and the heat values were evaluated to be 0.08 and 0.23 J, respectively. When the amount of electrolyte increased from 2 to 3 μl, an overlapped peak at around 300 °C became distinct and slightly shifted to a lower temperature. Compared to the results of the electrolyte [4,5], the peak temperature was much higher and the heat value was much less. In addition, no noticeable peak was found in the DSC curve of pristine Fe powder as shown in Fig. 7a. Hence, the exothermic peak at around 300 °C was involved in the reaction between Fe powder and electrolyte. With a further increase of the coexisting electrolyte from 3 to 4 and 5 μl, the two overlapped peaks became closer, and shifted downwards to 290 °C. The heat values were evaluated as 1.50 and 2.10 J when the amount of coexisting electrolyte was 4 and 5 μl, respectively. At this time, electrolyte decomposition was suspected to occur in addition to the reaction between Fe powder and electrolyte. On the other hand, comparing Fig. 7 with the results obtained from the discharged FeF_3 electrode in the conversion state with the electrolyte [6], the DSC curves were found to be similar: (1) the variational tendency of the exothermic peaks was quite similar when the ratio of electrolyte to active material was altered; (2) the exothermic reactions occurred in the same temperature range. Consequently, it was clear that Fe metal generated in the electrode at the conversion state had a direct effect on the thermal behavior of the discharged FeF_3 electrode.

Fig. 8 compares the heat values obtained from the mixtures of 0.3 mg Fe powder and given amounts of electrolyte and from the electrolyte alone. The heat values in Fig. 8 were evaluated by integrating DSC curves in the range of 250–360 °C, because the dominant exothermic reactions occurred in this range. The heat values obtained from the mixtures of 0.3 mg Fe powder and given amounts of electrolyte are marked with the circle points, while the heat values of electrolyte are shown by square points. For comparison, the data of 1 mg discharged FeF_3 electrode in the conversion state together with given amounts of the electrolyte, which was reported previously [6], is marked with triangle points and shown in Fig. 8. Linear fitting was carried out by the least-squares method. For the heat values of the mixtures of Fe powder and electrolyte, the slope of the lines changed at a break point on the electrolyte amount of 2.5 μl. This observation indicated that the dominant exothermic reaction of the mixtures was different before and after the break point. When the amount of coexisting electrolyte was more than 2.5 μl, the slope of the line for the mixtures was almost equal to that of the electrolyte alone. This result suggested that the amount of coexisting electrolyte was excess, and then thermally decomposed, which confirmed the reasoning for Fig. 7. In contrast, the electrolyte was not sufficient when the amount of electrolyte was less than 2.5 μl. As a result, some of the Fe powder remained from the reaction with electrolyte, and the exothermic heat was limited by the amount of electrolyte. Additionally, the heat values of the mixtures were much smaller than those of the electrolyte itself because of the reaction of Fe powder with the electrolyte. On the other hand, the variation trend of heat values for the Fe powder coexisting with the electrolyte was quite similar to that for the discharged FeF_3 electrode in the conversion state. The observed differences between them might be associated with the additives in the electrode, such as carbon and PTFE binder. Again, the generated Fe metal in the electrode was mainly responsible for the thermal behavior of discharged FeF_3 in the conversion state.

To further clarify the mechanism of the reaction between Fe powder and electrolyte, the effect of $LiPF_6$ on the thermal behavior of Fe powder in the electrolyte was investigated by DSC. Fig. 9 shows the DSC curve of a mixture of 0.3 mg Fe powder and 1 μl of EC + DMC solvent, together with that of a mixture of 0.3 mg Fe powder and 1 mg $LiPF_6$. The DSC curves of 0.3 mg Fe powder, 1 μl of EC + DMC solvent and 1 mg $LiPF_6$ are also shown as a reference in Fig. 9. When 1 mg of $LiPF_6$ powder was heated up alone, a small endothermic peak was observed at around 197 °C, followed by the other endothermic peak at around 290 °C. As reported by Ravdel et al. [28], the first peak and the second endothermic peak were attributed to the melting and the thermal decomposition of $LiPF_6$ ($LiPF_6$ (s) LiF (s) + PF_5 (g)), respectively. On the other hand, when Fe powder together with $LiPF_6$ was sealed in a pan, an exothermic peak at around 310 °C was observed in addition to the other two endothermic peaks at around 197 and 290 °C due to the melting and

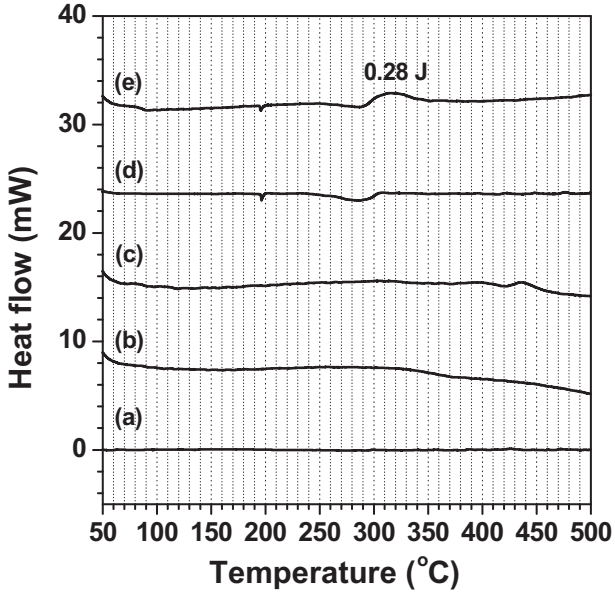

Fig. 9. DSC curves of (a) 0.3 mg Fe power, (b) 1 μl of EC + DMC solvent, (c) mixture of 0.3 mg Fe powder and 1 μl of EC + DMC solvent, (d) 1 mg $LiPF_6$, and (e) mixture of 0.3 mg Fe powder and 1 mg $LiPF_6$.

thermal decomposition of $LiPF_6$, respectively. This result clearly indicated that Fe powder could be reacted with PF_5 produced by $LiPF_6$ decomposition, and gave exothermic heat at around 310 °C. When Fe power was heated up in EC + DMC solvent, negligible small exothermic heat at temperatures above 380 °C was observed, while no exothermic peak was visible in DSC curve of EC + DMC solvent. Obviously, the solvent almost had no effect on the thermal stability of Fe powder in electrolyte. As reported by Kawamura et al. [29], PF_5 in the $LiPF_6$-based electrolyte may attack the electron lone pair of oxygen of a solvent molecule and then decompose. When Fe powder was heated up in the 1 M $LiPF_6$/EC + DMC electrolyte (Fig. 7), PF_5 in the electrolyte was consumed by the reaction with Fe powder. As a result, the electrolyte decomposition was suppressed and the decomposition temperature shifted to a higher temperature. Therefore, the heat generation of Fe powder with the electrolyte was smaller than the electrolyte alone (Fig. 8), due to the reaction of Fe powder with PF_5 in the electrolyte.

4. Conclusions

To identify the mechanism of exothermic reactions of a FeF_3 cathode in the electrolyte, the structure and thermal behavior of cycled FeF_3 electrodes were studied using a combination of XRD and DSC. The combination of XRD and DSC revealed that FeF_3 can be restored and the electrochemical was reversible even after the conversion reaction. In the discharged electrodes, a structural transformation to $LiFeF_3$ was observed after the 1Li insertion, and two compounds (Fe metal and LiF) were formed during the conversion reaction. Accordingly, the differences of thermal behavior in the electrolyte were presented in the DSC curves. On the other hand, the thermal behavior of LiF and Fe metal in the electrolyte was studied by DSC separately. It was clear that no reaction occurred between LiF and electrolyte even at elevated temperatures. In contrast, Fe powder was found to react with the electrolyte at around 300 °C, indicating that Fe metal generated in the electrode at the conversion state had a direct effect on the thermal behavior of the discharged FeF_3 electrode. In addition, Fe powder mixed with $LiPF_6$ was studied by DSC, and Fe powder was found to react with PF_5 produced by $LiPF_6$ decomposition. Therefore, the mixture of discharged FeF_3 electrode and electrolyte showed less heat generation than the electrolyte alone because some of the PF_5 in the electrolyte was consumed by the generated Fe metal in the electrode.

Acknowledgments

The present work was financially supported by the Li-EAD project of New Energy and Industrial Technology Development Organization, Japan.

References

[1] J. Yamaki, Y. Baba, N. Katayama, H. Takatsuji, M. Egashira, S. Okada, J. Power Sources 119–121 (2003) 789–793.
[2] T. Doi, M. Zhou, L. Zhao, S. Okada, J. Yamaki, Electrochem. Commun. 11 (2009) 1405–1408.
[3] T. Doi, L. Zhao, M. Zhou, S. Okada, J. Yamaki, J. Power Sources 185 (2008) 1380–1385.
[4] L. Zhao, M. Zhou, T. Doi, S. Okada, J. Yamaki, Electrochem. Acta 55 (2009) 125–130.
[5] M. Zhou, L. Zhao, T. Doi, S. Okada, J. Yamaki, J. Power Sources 195 (2010) 4952–4956.
[6] M. Zhou, L. Zhao, S. Okada, J. Yamaki, J. Power Sources 196 (2011) 8110–8115.
[7] S. Tobishima, J. Yamaki, J. Power Sources 81–82 (1999) 882–886.
[8] U.V. Sacken, E. Nodwell, A. Sundher, J.R. Dahn, J. Power Sources 54 (1995) 240–245.
[9] P.G. Balakrishnan, R. Ramesh, T.P. Kumar, J. Power Sources 155 (2006) 401–414.
[10] Y. Baba, S. Okada, J. Yamaki, Solid State Ionics 148 (2002) 311–316.
[11] F. Zhou, X. Zhao, J.R. Dahn, Electrochem. Commun. 11 (2009) 589–591.
[12] F. Zhou, X. Zhao, J.R. Dahn, J. Electrochem. Soc. 157 (7) (2010) A798–A801.
[13] F. Zhou, X. Zhao, A.J. Smith, J.R. Dahn, J. Electrochem. Soc. 157 (4) (2010) A399–A406.
[14] D.D. MacNeil, T.D. Hatchard, J.R. Dahn, J. Electrochem. Soc. 148 (7) (2001) A663–A667.
[15] D.D. MacNeil, J.R. Dahn, J. Electrochem. Soc. 148 (11) (2001) A1211–A1215.
[16] J.M. Tarascon, M. Armand, Nature 414 (2001) 367–395.
[17] I. Plitz, F. Badway, J. Al-Sharab, A. DuPasquier, F. Cosandey, G.G. Amatucci, J. Electrochem. Soc. 152 (2) (2005) A307–A315.
[18] G.G. Amatucci, N. Pereira, J. Fluorine Chem. 128 (2007) 243–262.
[19] H. Arai, S. Okada, J. Yamaki, J. Power Sources 68 (1997) 716–719.
[20] M. Nishijima, I.D. Gocheva, S. Okada, T. Doi, J. Yamaki, Y. Nishida, J. Power Sources 190 (2009) 558–562.
[21] F. Badway, N. Pereira, F. Cosandey, G.G. Amatucci, J. Electrochem. Soc. 150 (9) (2003) A1209–A1218.
[22] F. Badway, F. Cosandey, N. Pereira, G.G. Amatucci, J. Electrochem. Soc. 150 (10) (2003) A1318–A1327.
[23] H. Li, P. Balaya, J. Maier, J. Electrochem. Soc. 151 (11) (2004) A1878–A1885.
[24] N. Yamakawa, M. Jiang, B. Key, C.P. Grey, J. Am. Chem. Soc. 131 (2009) 10525–10536.
[25] S. Kim, D. Seo, H. Gwon, J. Kim, K. Kang, Adv. Mater. 22 (2010) 5260–5264.
[26] R.E. Doe, K.A. Persson, Y.S. Meng, G. Ceder, Chem. Mater. 20 (2008) 5274–5283.
[27] K. Mizushima, P.C. Jones, P.J. Wiseman, J.B. Goodenough, Mater. Res. Bull. 15 (1980) 783–789.
[28] B. Ravdel, K.M. Abraham, R. Gitzendanner, J. DiCarlo, B. Lucht, C. Campion, J. Power Sources 119–121 (2003) 805–810.
[29] T. Kawamura, A. Kimura, M. Egashira, S. Okada, J. Yamaki, J. Power Sources 104 (2002) 260–264.